Revealing the 120° Antiferromagnetic Néel Structure in Real Space: One Monolayer Mn on Ag(111)

C. L. Gao,[1] W. Wulfhekel,[1,2] and J. Kirschner[1]

[1]*Max-Planck-Institut für Mikrostrukturphysik Weinberg 2, 06120 Halle, Germany*

[2]*Physikalisches Institut, Universität Karlsruhe (TH), Wolfgang-Gaede Strasse 1, 76131 Karlsruhe, Germany*

(Received 6 October 2008; published 31 December 2008)

With spin-polarized scanning tunneling microscopy operating in the constant current mode, the 120° antiferromagnetic Néel structure was found for a monolayer Mn on Ag(111) in both fcc and hcp stacking. The existence of structurally equivalent, but magnetically distinguished, Mn islands was observed. While both the fcc and hcp Mn islands display the frustrated spin structure, the orientations of their magnetic moments differ by 30° possibly due to the spin-orbit coupling.

DOI: 10.1103/PhysRevLett.101.267205 PACS numbers: 75.70.Ak, 68.37.Ef, 75.50.Ee

Originating from the competing exchange interactions between neighboring atoms, frustrated spin structures are not only responsible for noncollinear antiferromagnetism but also play an important role in determining the exchange bias at the interface between ferromagnets and antiferromagnets [1]. Therefore, the investigation of noncollinear spin structures is both of fundamental interest and of technological importance [2]. A classical example of noncollinear antiferromagnetic spin structure is an arrangement of antiferromagnetic atoms in a two-dimensional (2D) hexagonal lattice. In this lattice, it is topologically impossible to align all nearest neighbors in an antiparallel fashion. Instead, a frustrated antiferromagnetic Néel structure as shown in Fig. 1(a) is stabilized. In this case, the magnetic moments are aligned with an angle of 120° between neighboring magnetic moments. The exclusive experimental observation of this noncollinear spin structure, however, has not been reported so far.

A 2D hexagonal arrangement of antiferromagnetic atoms is usually realized by growing a monolayer (ML) of magnetic atoms (e.g., Cr or Mn) on the hexagonal (0001) surfaces of hcp or (111) surfaces of fcc crystals. Extensive theoretical studies have been carried out which gave various and even contradictory results [3–7]. Spin structures from row-wise antiferromagnetic alignment [Cr/Cu(111) [4], Cr/Ag(111) [4], Mn/Cu(111) [4,5], Mn/Ag(111) [3]], double-row-wise antiferromagnetic structure [Mn/Ag(111) [4]], 120° Néel structure [Cr/Cu(111) [5], Mn/Cu(111) [6], Cr/Ag(111) [3]], or three-dimensional spin structure [Mn/Cu(111) [7]] have been predicted for the 2D hexagonal lattice. Even for the very same material system, the calculations of the ground state spin structure are not consistent. A direct experimental proof is highly needed to clarify the contradicting predictions.

With the development of spin-polarized scanning tunneling microscopy (SP-STM), it is possible to resolve antiferromagnetic spin structures on the atomic scale [8–11]. It has been proposed by Wortmann *et al.* [12] that, using SP-STM operating in the constant current mode, the collinear and noncollinear antiferromagnetic spin structures of a monolayer 2D antiferromagnet on fcc(111) surfaces can be distinguished experimentally. In this Letter, we followed the proposal of Wortmann *et al.* [12] and demonstrate that the frustrated 120° Néel structure is the ground state for one ML Mn on Ag(111) using STM with magnetically coated tips.

SP-STM operating in the constant current mode has demonstrated its ultimate resolution in many 2D antiferromagnetic systems, such as Mn/W(110) [8] and Fe/W(001) [9]. The very reason for the high spin resolution with magnetic tips has been well explained [12]. The presence of a magnetic supercell lowers the translational symmetry resulting in a significantly slower decay of the surface magnetic corrugation than the atomic corrugation. A constant current image taken with a magnetic tip reflects the magnetic supercell rather than the atomic unit cell. The magnetic contribution in the constant current SP-STM image is proportional to the projection of the spin polarization of the sample on the spin polarization of the tip [12]. In the case of the noncollinear Néel structure in Fig. 1(a), the projection of the magnetic moments on two orthogonal orientations as shown in Figs. 1(b) (the magnetization direction of the tip parallel to one of the moments) and 1(c) (the magnetization direction of the tip perpendicular to one of the moments) results in different SP-STM images [12].

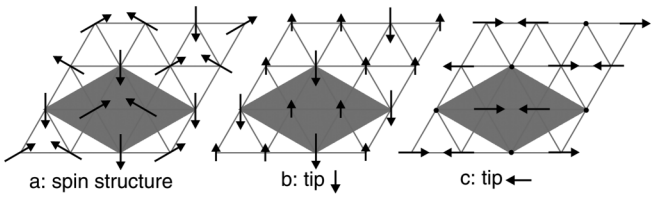

FIG. 1. 120° Néel antiferromagnetic structure in a hexagonal lattice (a) and the projection of the magnetic moments on the axis (b) parallel and (c) perpendicular to one atomic moment. The magnetic unit cell is indicated by the gray diamond.

The experiments were performed in ultrahigh vacuum. The Ag(111) single crystal was prepared by cycles of Ar^+ ion sputtering and annealing to 800 K. Mn was evaporated from an *e*-beam heated crucible and deposited on Ag(111) while keeping the substrate at 200 K which effectively hinders intermixing between Mn and Ag. The STM measurements were done with low temperature STM at 5 K. For the nonmagnetic measurements, a W tip was used, while, for the magnetic measurements, the W tip was coated with ≈ 70 ML of Cr which gives an in-plane spin sensitivity [13].

The first ML of Mn grows pseudomorphically on Ag(111). Low energy electron diffraction (LEED) showed (1×1) patterns excluding any kind of reconstruction. Figure 2(a) gives an overview of the topography of 0.6 ML Mn on Ag(111). Mn either grows along the Ag step edges [marked by the arrows in Fig. 2(a)] forming ML stripes or grows as ML triangular islands [see the line profile in Fig. 2(a)]. There are two possible adsorption sites that the Mn ML can occupy on the fcc(111) surface, i.e., the fcc site or the hcp site. The Mn stripes along the steps are on fcc sites because no dislocation was observed between Ag and Mn as shown in Fig. 2(d). The Mn islands fall into two classes: Most of them point up (up islands), and a few of them point down (down islands).

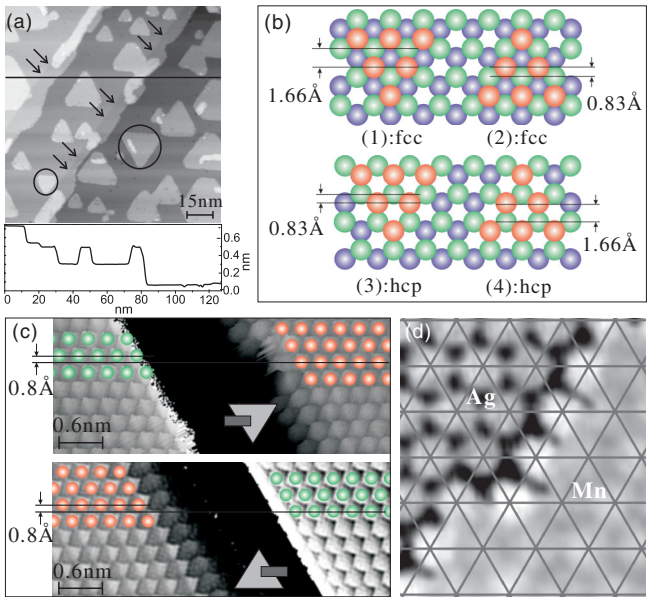

FIG. 2 (color). (a) Topography of 0.6 ML Mn on Ag(111) together with a section profile. $U_{\text{bias}} = 0.23$ V; $I_t = 20$ nA. The arrows indicate Ag substrate step edges. While most Mn islands point upwards, a few of them point downwards as marked by the circles. (b) Four possible types of Mn ML triangular islands on Ag(111). Red represents the Mn atoms, green and blue the atoms of the first and second Ag layer, respectively. The two fcc (hcp) islands are distinguished by their step edge orientations and the lateral displacements between the Mn atomic rows and the Ag atom rows measuring towards the base of the triangular from Mn to Ag. (c) The atomically resolved topographic images on both the Mn (red) island and the Ag (green) substrate for islands pointing up and pointing down. $U_{\text{bias}} = 15$ mV; $I_t = 20$ nA. (d) The atomically resolved topographic image close to the Ag step where the growth of Mn along the Ag step is clearly visible. No dislocation is present between Ag and Mn as shown by the lattice grid. $U_{\text{bias}} = 2$ mV; $I_t = 10$ nA.

There are four possible ways for Mn to form ML triangular islands on Ag(111) as sketched in Fig. 2(b): fcc and hcp stacked islands with two types of closed packed step edges each. One of each two fcc (hcp) islands points up, and the other points down. In the experiment, we obtained atomic resolution simultaneously on the Ag substrate and on the Mn islands for both the up and down islands as shown in Fig. 2(c). If we measure the lateral displacement between the atomic rows of the up and down islands and the Ag substrate in the direction towards the triangular base of the island, both are 0.8 Å, indicating that the two types of islands are of opposite stacking [i.e., in agreement with Figs. 2(b)(2) and 2(b)(3)]. We, however, cannot determine which one is fcc and which one is of hcp stacking with solely this measurement, as we only combined information of the Mn layer and the topmost Ag layer. The latter shows, however, a sixfold symmetry in our STM images. Thus we cannot distinguish with STM between the two configurations that are rotated by 180°, i.e., a situation where up and down islands are exchanged. This means either the up islands are on fcc sites and the down islands are hcp islands or vice versa. It is, however, not clear which one is on fcc sites and which one is on hcp sites. This will be clarified in the following discussion by combining with the spin resolved measurements.

In Fig. 2(c), the STM images were taken with W tips and only a (1×1) atomic arrangement was observed. With Cr coated tips, the constant current images on the Mn islands differ from the (1×1) structure. We first focus on the majority islands (up islands). With a fixed tip magnetization, we observed images as shown in Fig. 3(b). The left image of Fig. 3(b) is characterized by bright protrusions forming $(\sqrt{3} \times \sqrt{3})$ reconstruction. When the tip is moved from island to island, the image either stays the same or reverses in contrast as depicted in the right image of Fig. 3(b). In the SP-STM experiments, a notorious problem is the uncontrollable spin polarization of the tip apex. In our case, the Cr coated tips have an in-plane spin sensitivity, while the in-plane direction is undetermined. By removing a small amount of Cr from the tip with voltage pulses, one may eventually alter the in-plane spin sensitive direction which gives another series of constant current images as given in Fig. 3(c). The images are characterized by bright, intermediate, and dark areas which again form a $(\sqrt{3} \times \sqrt{3})$ reconstruction. A reversal of the contrast was observed when moving the tip from one island to another. Since both the LEED pattern and the atomically resolved topographic images taken with W tips exclude any kind of

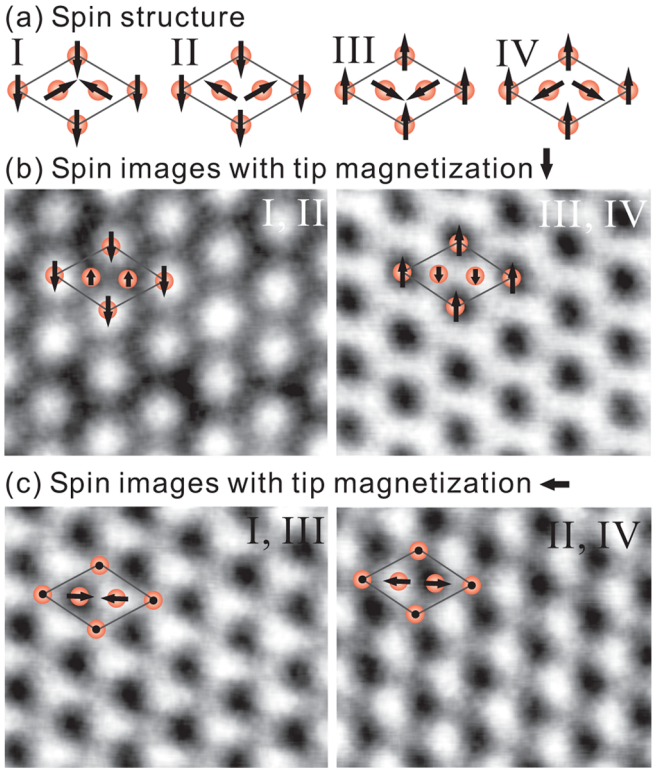

FIG. 3 (color online). (a) Four possible configurations of the 120° Néel structure (modulo a 120° rotation of all spins in the same sense). (b) and (c) are two groups of constant current images taken with magnetic tips. The size of the images is about 2×2.5 nm^2. $U_{\text{bias}} = 20$ mV; $I_t = 20$ nA. The magnetic unit cells are marked in the images together with the projection of the sample spin polarization onto the tip spin polarization direction. By assuming a magnetic orientation of the tip, the projections of the four domains in (a) on the tip magnetization direction result in different magnetic images. All of the images were taken on the up islands.

crystallographic reconstruction or intermixing on the surface, the observed $(\sqrt{3} \times \sqrt{3})$ reconstruction is of magnetic origin. The corrugation Δz (magnetic contrast) varies between 5 and 15 pm depending on the status of the tip and the bias voltage. Both the size of the magnetic contrast and the pattern of Figs. 3(b) and 3(c) agree perfectly with the theoretical prediction for SP-STM images of a 120° Néel structure by Wortmann *et al.* [12] with the magnetization direction of the tip parallel to one of the moments of Mn in Fig. 3(b) and perpendicular in Fig. 3(c). In Figs. 3(b) and 3(c), the corresponding projection of the 120° Néel structure on the tip magnetization direction was given with the $(\sqrt{3} \times \sqrt{3})$ reconstruction unit cell. Other spin configurations (e.g., row-wise antiferromagnetic order) do not agree with the observed patterns. Thus, it can be concluded that single ML Mn islands (up islands) on Ag(111) have a 120° Néel structure.

The reversal of spin contrast when moving the tip from one island to another island can be explained by the existence of different magnetic domains in Mn islands. If we consider only the free hexagonal ML Mn of 120° Néel structure excluding the influence of the substrate and assuming a spin direction along a high symmetry direction, four energetically degenerate domains exist as sketched in Fig. 3(a). These four domains give all possible structures modulo a rotation of all spins by an angle of 120° [14]. If the tip magnetization is parallel to one of the Mn moments, the projection of domains I and II on the tip magnetization direction gives the left image of Fig. 3(b), and domains III and IV give the right image of Fig. 3(b). If the tip magnetization is perpendicular to one of the Mn moments, the projection of domains I and III on the tip magnetization direction gives the left image of Fig. 3(c), and domains II and IV give the right image of Fig. 3(c). Because of the maximal 30° difference in magnetization direction between the different theoretical spin arrangements and the tip spin polarization, the observed constant current images for a STM tip of arbitrary in-plane spin polarization direction are either close to Fig. 3(b) or close to Fig. 3(c). In order to explain all of the SP-STM images in Figs. 3(b) and 3(c), a combination of the theoretical domains I and IV (or II and III) together with an arbitrary spin polarization direction of the tip is sufficient. This means that it is not clear whether all four domains in Fig. 3(a) are present at the surface. The Mn atoms are, however, coupled to the Ag crystal, which is only of threefold rotational symmetry implying that the four domains in Fig. 3(a) are not equivalent anymore but may differ in energy due to the spin-orbit interaction. The probability of finding either of the inverted contrasts in images with a fixed tip magnetization, however, was the same. This indicates that the energy difference between I and IV (or II and III) is negligible in agreement with an expected sixfold in-plane magnetocrystalline anisotropy.

Theoretical calculations have predicted either a row-by-row antiferromagnetic structure [3] or a two-row-by-two-row antiferromagnetic structure [4] for Mn/Ag(111). They do not agree with our experimental observation of the 120° antiferromagnetic Néel structure. Considering the contradictory theoretical predictions about spin structure of Cr and Mn ML on fcc(111) substrates [3–7], an improvement of theory is highly needed.

The above discussion focused on the majority islands (up islands). The down islands show exactly the same behavior as the up islands indicating that the down islands have the same 120° Néel structure. To conclude, using a tip with fixed magnetization direction, all islands behave according the following rules: Up islands display patterns that differ only by an inversion of contrast; i.e., they are either of Fig. 3(b) or of Fig. 3(c). Down islands display the same behavior. If one wants to observe a change of images from Figs. 3(b) and 3(c) within the same type of islands, one has to change the magnetization direction of the tip. A change from the pattern of Figs. 3(b) and 3(c) or vice versa,

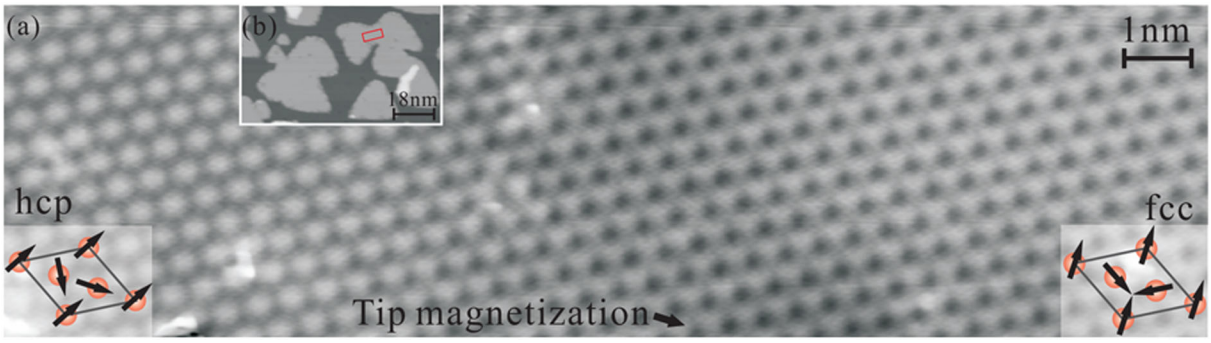

FIG. 4 (color online). (a) Spin image of the rectangular area in (b). $U_{\text{bias}} = 20$ mV; $I_t = 20$ nA. The right part is the hcp region, and the left part is the fcc region. In the middle, the image appears darker which is considered as the smooth structural transition region from hcp to fcc. With the assumed tip magnetization orientation, one possible configuration of the 120° Néel structure is given. (b) Topography of submonolayer Mn. Islands are connected together.

however, was always observed when moving the tip of fixed magnetization from the up islands to down islands. This implies that Mn islands on fcc sites and on hcp sites have different magnetic anisotropy that determines the orientations of the Mn moments. When moving the tip from the up islands to the Mn stripes along the Ag step edges, the spin image stays the same or reverses its contrast. This indicates that Mn stripes and the up islands belong to the same type of structure. Since there is no dislocation at the Ag step between Ag and Mn [Fig. 2(d)], the Mn stripes and the up islands are of fcc stacking, while the down islands are of hcp stacking.

The different magnetic anisotropy between fcc and hcp islands comes from the different spin-orbit coupling with the Ag substrate which intrinsically determines the easy direction of the Mn moments on fcc and hcp sites. This can be more clearly seen when up and down islands are connected as shown Fig. 4. Zooming into the connection area with a magnetic tip, the hcp region (down island) appears as Fig. 3(b), while the fcc region (up island) appears as Fig. 3(c). This can be explained only if the Mn moments rotate by 30° as shown in the sketch in the figure with the assumed tip magnetization direction [15]. The transition from hcp to fcc is smooth which can be thought as a structural domain wall accompanied with a change of magnetic orientation. The transition region appears darker (in the middle of the image) in the constant current image with a width of a few nanometers. A smooth structural transition from hcp to fcc was also reported for the Au(111) surface [16]. A sharp magnetic domain wall in antiferromagnetic materials is not preferred since it must overcome the large exchange energy. Antiferromagnetic domains are usually accompanied with structural variation [17] or local defects [9]. In our case, domain walls were observed only in the presence of the structural transition between hcp and fcc stacking.

In conclusion, we have demonstrated the 120° Néel structure of monolayer Mn on Ag(111). Both Mn on fcc and hcp atomic sites are found with the same spin structure but with different orientation of the individual moments. While we do not know the exact orientation of the in-plane spin sensitive direction of the tip such that the orientation of the moments cannot be exclusively determined, we can conclude that the orientation of the Mn moments differs by 30° between fcc and hcp stacked islands. The different orientation of the Mn moments is most likely due to different easy directions of magnetization caused by the different spin-orbit coupling for the two stackings. A disagreement with the previous theoretical predictions indicates that a careful reinvestigation is needed in theory.

[1] R. L. Stamps, J. Phys. D **33**, R247 (2000).
[2] W. Kuch *et al.*, Nature Mater. **5**, 128 (2006).
[3] S. Heinze *et al.*, Appl. Phys. A **75**, 25 (2002).
[4] P. Krüger, M. Taguchi, and S. Meza-Aguilar, Phys. Rev. B **61**, 15 277 (2000).
[5] P. Kurz, G. Bihlmayer, and S. Blügel, J. Appl. Phys. **87**, 6101 (2000).
[6] D. Spišák and J. Hafner, Phys. Rev. B **61**, 12 728 (2000).
[7] P. Kurz *et al.*, Phys. Rev. Lett. **86**, 1106 (2001).
[8] M. Bode *et al.*, Nature (London) **447**, 190 (2007).
[9] M. Bode *et al.*, Nature Mater. **5**, 477 (2006).
[10] C. L. Gao *et al.*, Phys. Rev. Lett. **98**, 107203 (2007).
[11] C. L. Gao *et al.*, Phys. Rev. Lett. **100**, 237203 (2008).
[12] D. Wortmann *et al.*, Phys. Rev. Lett. **86**, 4132 (2001).
[13] A. Wachowiak *et al.*, Science **298**, 577 (2002).
[14] Note that a rotation of all spins by 120° is equivalent to a translation by a lattice vector and that patterns I and IV as well as patterns II and III are related by a rotation of all spins by 60°.
[15] Note that the structures of Figs. 3(b) and 3(c) are related by a rotation of the tip spin polarization by 90° which is equivalent to a rotation of all sample spins by 30° modulo the aforementioned invariance of the patterns by a rotation of 120°.
[16] J. A. Stroscio *et al.*, J. Vac. Sci. Technol. A **10**, 1981 (1992).
[17] N. B. Weber *et al.*, Phys. Rev. Lett. **91**, 237205 (2003).